

Physalin A induces G2/M phase cell cycle arrest in human non-small cell lung cancer cells: involvement of the p38 MAPK/ROS pathway

Ning Kang^{1,2} · Jun-feng Jian⁵ · Shi-jie Cao⁴ · Qiang Zhang¹ · Yi-wei Mao⁵ · Yi-yuan Huang¹ · Yan-fei Peng¹ · Feng Qiu³ · Xiu-mei Gao²

Received: 3 November 2015 / Accepted: 12 March 2016 / Published online: 21 March 2016
© Springer Science+Business Media New York 2016

Abstract Physalin A (PA) is an active withanolide isolated from *Physalis alkekengi* var. *franchetii*, a traditional Chinese herbal medicine named Jindenglong, which has long been used for the treatment of sore throat, hepatitis, and tumors in China. In the present study, we firstly investigated the effects of PA on proliferation and cell cycle distribution of the human non-small cell lung cancer (NSCLC) A549 cell line, and the potential mechanisms involved. Here, PA inhibited cell growth in dose- and time-

dependent manners. Treatment of A549 cells with 28.4 μM PA for 24 h resulted in approximately 50 % cell death. PA increased the amount of intracellular ROS and the proportion of cells in G2/M. G2/M arrest was attenuated by the addition of ROS scavenger NAC. ERK and P38 were triggered by PA through phosphorylation in a time-dependent manner. The phosphorylation of ERK and P38 were not attenuated by the addition of NAC, but the use of the p38 inhibitor could reduce, at least in part, PA-induced ROS and the proportion of cells in G2/M. PA induces G2/M cell cycle arrest in A549 cells involving in the p38 MAPK/ROS pathway. This study suggests that PA might be a promising therapeutic agent against NSCLC.

Keywords Physalin A · G2/M cell cycle arrest · p38 · Reactive oxygen species (ROS) · Non-small cell lung cancer (NSCLC)

✉ Feng Qiu
fengqiu20070118@163.com

✉ Xiu-mei Gao
gaoxiumei@tjutc.edu.cn

¹ School of Integrative Medicine, Tianjin University of Traditional Chinese Medicine, 312 Anshanxi Road, Nankai District, Tianjin 300193, People's Republic of China

² Tianjin State Key Laboratory of Modern Chinese Medicine, Tianjin University of Traditional Chinese Medicine, 312 Anshanxi Road, Nankai District, Tianjin 300193, People's Republic of China

³ College of Traditional Chinese Medicine, Tianjin University of Traditional Chinese Medicine, 312 Anshanxi Road, Nankai District, Tianjin 300193, People's Republic of China

⁴ Department of Natural Products Chemistry, Shenyang Pharmaceutical University, 103 Wenhua Road, Shenyang 110016, People's Republic of China

⁵ Department of Biochemistry and Molecular Biology, Shenyang Pharmaceutical University, 103 Wenhua Road, Shenyang 110016, People's Republic of China

Abbreviations

ANOVA	Analysis of variance
DCF-DA	2',7'-Dichloro -fluorescein diacetate
DMSO	Dimethyl sulfoxide
FBS	Fetal bovine serum
iNOS	Inducible nitric oxide synthase
LSD	Least significant difference
MAPKs	Mitogen-activated protein kinases
MPF	Mitosis-promoting factor
MTT	3-(4,5-Dimethylthiazol-2-yl)-2,5-diphenyltetrazolium bromide
NAC	N-Acetylcysteine
NO	Nitric oxide
NSCLC	Non-small cell lung cancer
PA	Physalin A
PI	Propidium iodide
ROS	Reactive oxygen species

Introduction

Lung cancer is a leading cause of cancer-related mortality in both men and women [1]. Age-adjusted incidence of lung cancer is 84.9 per 100,000 men and 55.6 per 100,000 women [1]. It has a dismal prognosis with 5-year relative survival rates of only 13.6–37 % [1]. Non-small cell lung cancer (NSCLC) accounts for almost 80 % of lung cancer cases [2]. Surgical treatment used alone often fails due to cancer cell dissemination [3]. Although chemotherapy is appropriate for many patients with lung cancer, it is increasingly recognized that traditional chemotherapeutic agents have reached a therapeutic plateau [4]. Therefore, novel anticancer drugs are needed.

Conventional chemotherapies decrease not only the proliferation of cancer cells, but also the proliferation of actively proliferating normal cells by inducing cell cycle checkpoint arrest. DNA damages occurring during the G1 phase induce G1/S arrest, while DNA damages occurring during the G2 phase prevent the cell from entering the M phase [5]. Proliferation can be resumed once the damage is repaired; if the repair fails, it will result in deleterious mutations, potentially leading to cell death [6]. Cancer cells often have defective checkpoints and rely on other mechanisms to continue proliferating [7]. These other mechanisms may be targeted by new drugs [8]. Since the defective checkpoints are specific to the cancer, novel agents targeting specifically these checkpoints should spare normal cells [8]. Therefore, targeting the defective cell cycle checkpoints is an appropriate strategy against cancer [8], but a better understanding of these checkpoints is still necessary.

Mitogen-activated protein kinases (MAPKs) play a number of key roles in the transduction of extracellular signals into cellular responses. In mammalian cells, three MAPK families have been clearly characterized: ERK, JNK, and p38 [9]. MAPK pathways relay, amplify, and integrate signals from a diverse range of stimuli to elicit responses such as cellular proliferation, differentiation, development, and inflammation. MAPK activation at G1 is correlated with the ability to enter S phase [10]. VEGF induces G1/S progression and cell proliferation through ERK to JNK cross-activation and subsequent JNK action [11]. p38 is involved in the differentiation of different cell types such as adipocytes, erythroblasts, and myoblasts [12]. Activated p38 can cause mitotic arrest in somatic cell cycle at the spindle assembly checkpoint [13]. Therefore, a better understanding of the relationship between the MAPK signal transduction system and the regulation of cell cycle progression is essential for the rational design of novel therapeutic approaches targeting the cell cycle checkpoints.

Reactive oxygen species (ROS) (hydroxyl radicals, superoxide anions, singlet oxygen, and hydrogen peroxide)

are generated as by-products of cellular metabolism [14]. Increases in intracellular ROS have been detected in a variety of cells stimulated with cytokines, growth factors, and anticancer drugs. ROS may function as intracellular messengers modulating signaling pathways, protein kinases, and transcription factors [15]. Excessive ROS generation can result in oxidative stress, loss of cell function, cell cycle arrest, and apoptosis [16]. An accumulation of ROS can severely damage cellular macromolecules, especially DNA, and induce cell cycle arrest [17].

Physalin A (PA) is an active withanolide isolated from *Physalis alkekengi* var. *franchetii* (Solanaceae) (Chinese name: “Jindenglong”) and is found in high concentrations in the plant [18]. The calyx of this plant has been commonly used as a traditional Chinese medicine for the treatment of cough, sore throat, hepatitis, and tumors [19]. PA was reported to induce apoptosis on prostate cancer cells via JNK and ERK activation [18]. Previous studies by our group revealed that apoptosis induced by PA in HT1080 cells was associated with upregulation of caspase-3 and caspase-8 expression and that autophagy induced by PA was found to antagonize apoptosis in HT1080 cells [20]. Our previous studies showed that PA induces the inducible nitric oxide (NO) synthase (iNOS) and the generation of NO promoted both apoptosis and autophagy of A375-S2 cells [21] and that PA also induces the generation of reactive oxygen species, leading to apoptosis in A375-S2 cells [6]. Especially, PA did not show inhibitory effects on normal human cells (human peripheral blood mononuclear cells) [20] and has a lower toxicity than 5-fluorouracil or paclitaxel on normal human cells [20]. Therefore, PA could be considered a promising agent for the treatment of cancer.

However, no study has reported the effects of PA on human NSCLC cells and thus the mechanisms remain unknown. Therefore, the aim of the present study was to assess the effects of PA on NSCLC A549 cell proliferation, cell cycle distribution, and the potential mechanisms involved. Results could have an important significance for the use of PA as a new anticancer drug against NSCLC.

Materials and methods

Reagents

PA was isolated from *Physalis alkekengi* var. *franchetii* at the Department of Natural Products Chemistry (Shenyang Pharmaceutical University) according to published method [22] and was identified by comparing its physical and spectroscopic (^1H NMR and ^{13}C NMR) data with those reported in the literature [23]. Figure 1a presents its chemical structure. The purity was measured by HPLC

[column: Agilent Zorbax SB-C18, 4.6 × 150 mm, 5 μm; solvent phase: methanol-H₂O (60:40)] and was determined to be 98.0 % pure. PA was dissolved in dimethyl sulfoxide (DMSO) to make a stock solution and diluted using DMEM (GIBCO, Invitrogen Inc., Carlsbad, CA, USA) before the experiments. DMSO concentration in all cell cultures was kept below 0.001 %. Fetal bovine serum (FBS) was obtained from TBD Biotechnology Development (Tianjin, China); 3-(4,5-dimethylthiazol-2-yl)-2,5-

diphenyltetrazolium bromide (MTT), propidium iodide (PI), JNK inhibitor SP600125, ERK inhibitor PD98059, p38 inhibitor SB203580, ROS scavenger *N*-acetylcysteine (NAC), 2',7'-dichlorofluorescein diacetate (DCF-DA), PMSF, aprotinin, and leupeptin were purchased from Sigma Chemical (St Louis, MO, USA). Polyclonal antibodies against ERK, p-ERK, p38, p-p38, p53, p-p53, p21, Cdc25C, p-Cdc25C, Cdc2, p-Cdc2, cyclin B1, β-actin, and horseradish peroxidase-conjugated secondary antibodies

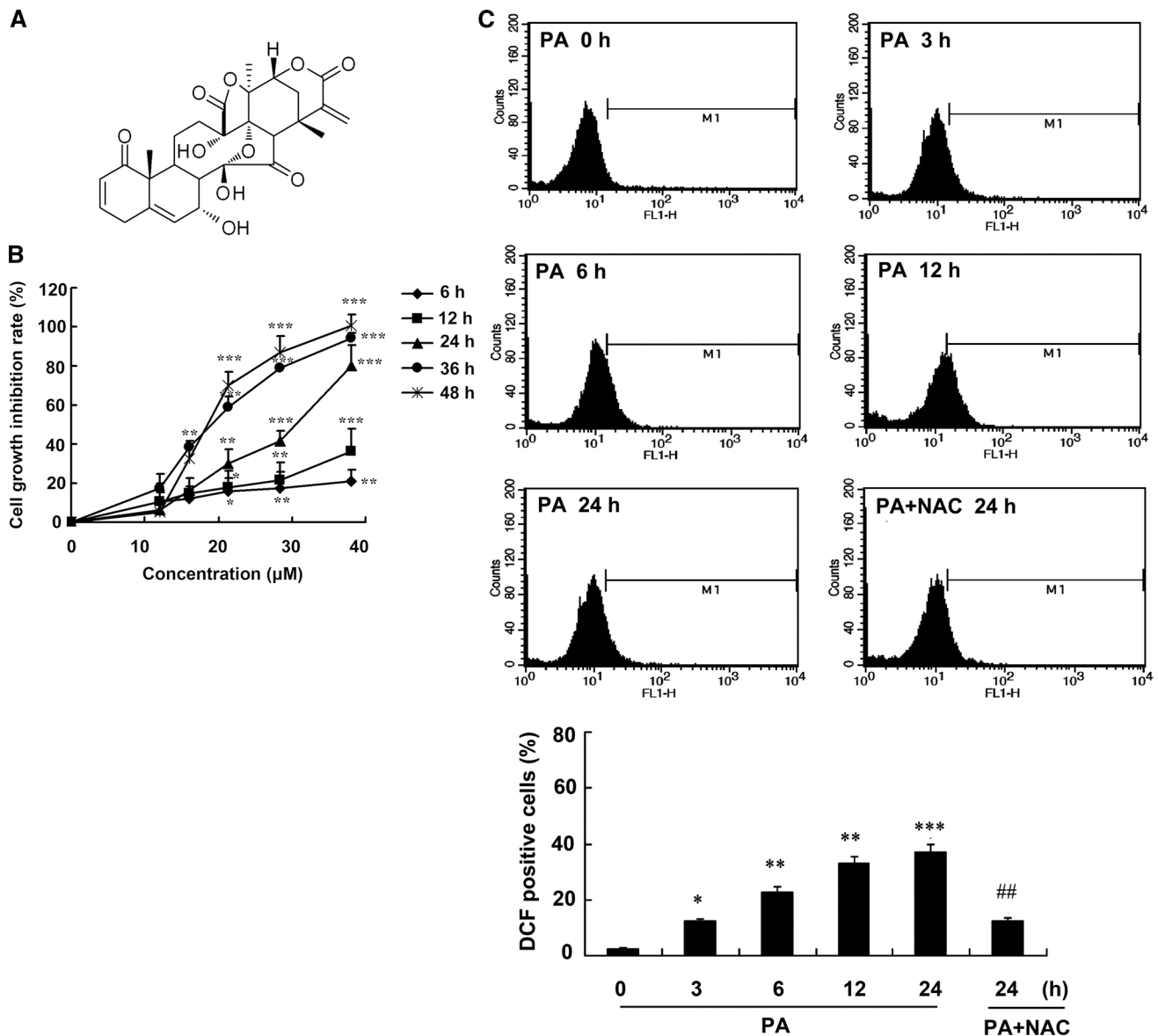


Fig. 1 Physalin A (PA) induced growth inhibition and reactive oxygen species (ROS) generation in human non-small-cell lung cancer A549 cell. **a** Chemical structure of PA. **b** A549 cells were treated with various doses (0, 12, 16, 21.3, 28.4, and 38 μM) of PA for 3, 6, 12, and 24 h. Cell growth inhibition rate (%) was measured using the MTT assay. Data are shown as mean ± standard deviation (SD) from three independent experiments. * $P < 0.05$, ** $P < 0.01$, *** $P < 0.001$ versus controls (0 μM PA) at the same time point.

c A549 cells were cultured with 28.4 μM PA for 0, 3, 6, 12, and 24 h in the absence or presence of 3 mM *N*-acetylcysteine (NAC), the ROS scavenger. The generation of ROS was measured by flow cytometry using the ROS-detecting fluorescent dye DCF-DA. Data are shown as mean ± SD from three independent experiments. * $P < 0.05$, ** $P < 0.01$, and *** $P < 0.001$ versus control group (28.4 μM PA for 0 h); ### $P < 0.01$ versus A549 cells treated with 28.4 μM PA for 24 h

were obtained from Santa Cruz Biotechnology (Santa Cruz, CA, USA). The material under study is endotoxin free.

Cell culture and treatment

Human NSCLC A549 cells were obtained from the American Type Culture Collection (ATCC; Manassas, VA, USA) and were cultured in DMEM supplemented with 10 % FBS, 2 mM L-glutamine (GIBCO, Invitrogen Inc., Carlsbad, CA, USA), 100 kU/L penicillin, and 100 mg/L streptomycin at 37 °C in 5 % CO₂. Cells in the exponential phase were used in the experiments.

A549 cells were treated with 28.4 μM PA for 0, 3, 6, 12, or 24 h or pretreated with 3 mM NAC, 2.5 μM PD98059, 5.0 μM SB203580, or 2.5 μM SP600125 for 1 h and then treated with 28.4 μM PA for 24 h.

Cytotoxicity assay

A549 cells were incubated in 96-well plates at a density of 8×10^5 cells/well. After treatment with drugs, the cytotoxic effect was measured using the MTT assay [24] and the results were read using a microplate spectrophotometer (TECAN SPECTRA; Tecan Group Ltd., Männedorf, Switzerland) at 492 nm [25]. The blank control contained medium without cells. Cell growth inhibition rate (%) was calculated as: $[1 - (A492_{\text{experiment group}} - A492_{\text{blank}}) / (A492_{\text{negative control}} - A492_{\text{blank}})] \times 100 \%$.

Cell cycle distribution by flow cytometry

After treatment with drugs, 1×10^6 cells were harvested, washed with PBS, and fixed in 70 % ethanol at 4 °C for at least 12 h. After removing the ethanol and washing with PBS, the resuspended cells were stained with the fluorescent probe solution containing 50 μg/mL PI and 1 mg/mL DNase-free RNaseA for 30 min on ice in the dark. DNA fluorescence of PI-stained cells was evaluated by a FACScan flow cytometer (BD Biosciences, Franklin Lake, NJ, USA). A minimum of 10,000 events were analyzed per sample. The DNA histograms were gated and analyzed using the Modfit software on a Mac workstation to estimate the percentage of cells in the various phases of the cell cycle (subG1, G0/G1, S, and G2/M).

Intracellular ROS generation analysis by flow cytometry

Intracellular ROS accumulation was detected by flow cytometry using the cell-permeable fluorogenic probe DCF-DA. After treatment with drugs, culture supernatants were removed, and the cells were then incubated with 10 μM DCF-DA in fresh medium at 37 °C for 1 h in the

dark. After incubation, the culture medium was removed, and the cells were then washed with cold PBS buffer. Then, the cells were harvested and the pellets were suspended in 500 μl of PBS. Samples were analyzed at an excitation wavelength of 480 nm and an emission wavelength of 525 nm by a FACScan flow cytometer.

Western blot analysis

After treatment with drugs, cells were collected and Western blot was carried out as previously described [26] with some modifications. Cell pellets were resuspended in lysis buffer (50 mM Hepes pH 7.4, 1 % Triton-X100, 2 mM sodium orthovanadate, 100 mM sodium fluoride, 1 mM edetic acid, 1 mM PMSF, 10 μg/mL of aprotinin, and 10 μg/mL of leupeptin) and lysed on ice for 30 min. After centrifugation at $14,000 \times g$ for 10 min at 4 °C, the protein content of the supernatant was determined using a protein assay reagent (Bio-Rad, Hercules, CA, USA). The protein lysates (50 μg) were separated by electrophoresis in 12 % SDS polyacrylamide gels and blotted onto nitrocellulose membrane (Amersham Biosciences, Piscataway, NJ, USA). The membranes were blocked with blocking buffer (5 % skimmed milk). Proteins were detected with the primary antibodies against ERK, p-ERK, p38, p-p38, p53, p-p53, p21, Cdc25C, p-Cdc25C, Cdc2, p-Cdc2, cyclin B1, and β-actin, followed by HRP-conjugated secondary antibody, and visualized using ECL (Sigma, St Louis, MO, USA). Immunoreactive bands were quantified using the Image J analysis software (National Institutes of Health, Bethesda, MD, USA). Quantification of protein expression levels was expressed as relative folds compared to the control group.

Statistical analysis

All statistical analyses were conducted using SPSS 17.0 (IBM, Armonk, NY, USA). Data are expressed as mean ± standard deviation (SD) of three independent experiments. Statistical significance was evaluated by one-way analysis of variance (ANOVA) with the Least Significant Difference (LSD) test for post hoc analysis. $P < 0.05$ was considered statistically significant.

Results

Cytotoxic effect of PA against A549 cells

To detect the cytotoxic effects of PA on A549 cells, the cells were cultured with different concentrations of PA for 6, 12, 24, 36, and 48 h. PA-induced cell growth inhibition in dose- and time-dependent manners (Fig. 1b), producing

IC50 values of 111.85 ± 7.21 , 63.32 ± 4.58 , 28.41 ± 3.84 , 20.49 ± 4.10 , and $18.16 \pm 1.72 \mu\text{M}$ for PA treatments of 6, 12, 24, 36, and 48 h, respectively.

PA induced generation of ROS in A549 cells

Recent evidence indicated that intracellular ROS over-accumulation may mediate cell death [27]. In this study, after A549 cells were exposed to $28.4 \mu\text{M}$ PA for 0, 3, 6, 12, or 24 h, moderate generation of ROS were observed at 3 h and the level of ROS was increased significantly at 24 h. The ratio of DCF-DA-positive cells was 2.55, 12.32, 22.85, 32.85, and 36.87 % at 0, 3, 6, 12, and 24 h, respectively (all $P < 0.05$). As expected, the ROS scavenger NAC at 3 mM markedly decreased the levels of ROS from 36.87 to 12.41 % at 24 h ($P < 0.01$) (Fig. 1c).

PA induced G2/M cell cycle arrest in A549 cells and this effect was alleviated by ROS scavenger NAC

It was reported that ROS are involved in cell cycle arrest [27]. In present study, the ROS scavenger NAC could alleviate cell growth inhibition in PA-treated cells. Pre-incubation with 3 mM NAC effectively rescued growth inhibition from 45.2 % for PA alone to 7.1 % in the presence of NAC (Fig. 2a). Then, A549 cells were exposed to $28.4 \mu\text{M}$ PA for 0, 3, 6, 12, and 24 h. The ratio of G2/M phase was 21.05, 29.55, 34.08, 35.43, and 40.55 % at 0, 3, 6, 12, and 24 h, respectively (all $P < 0.01$); there was no difference in the proportions of cells in the S phase, and the proportions of cells in the G0/G1 phase were reduced. When incubated with the ROS scavenger NAC at 3 mM, the percentage of the G2/M phase was reduced from 40.55 to 25.43 % at 24 h ($P < 0.01$) (Fig. 2b).

Phosphorylation of ERK and P38 were not attenuated by the addition of NAC in A549 cells

The MAPK family members, including ERK, JNK, and p38, play important roles in the regulation of cell proliferation [28]. Here, the MTT assay showed that the cell growth inhibition ratio in PA-treated cells was reduced from 41.25 % to 38.7 % ($P < 0.05$) for $2.5 \mu\text{M}$ of PD98059 and to 38.3 % ($P < 0.05$) for $5 \mu\text{M}$ of SB203580. However, SP600125 had no significant effect on PA-treated cells, suggesting that JNK was not involved in mediating PA-induced cell growth inhibition (Fig. 3a).

Since PD98059 and SB203580 were found to be able to reverse PA-triggered cell growth inhibition, ERK and p38 might be essential downstream effectors of PA. Therefore,

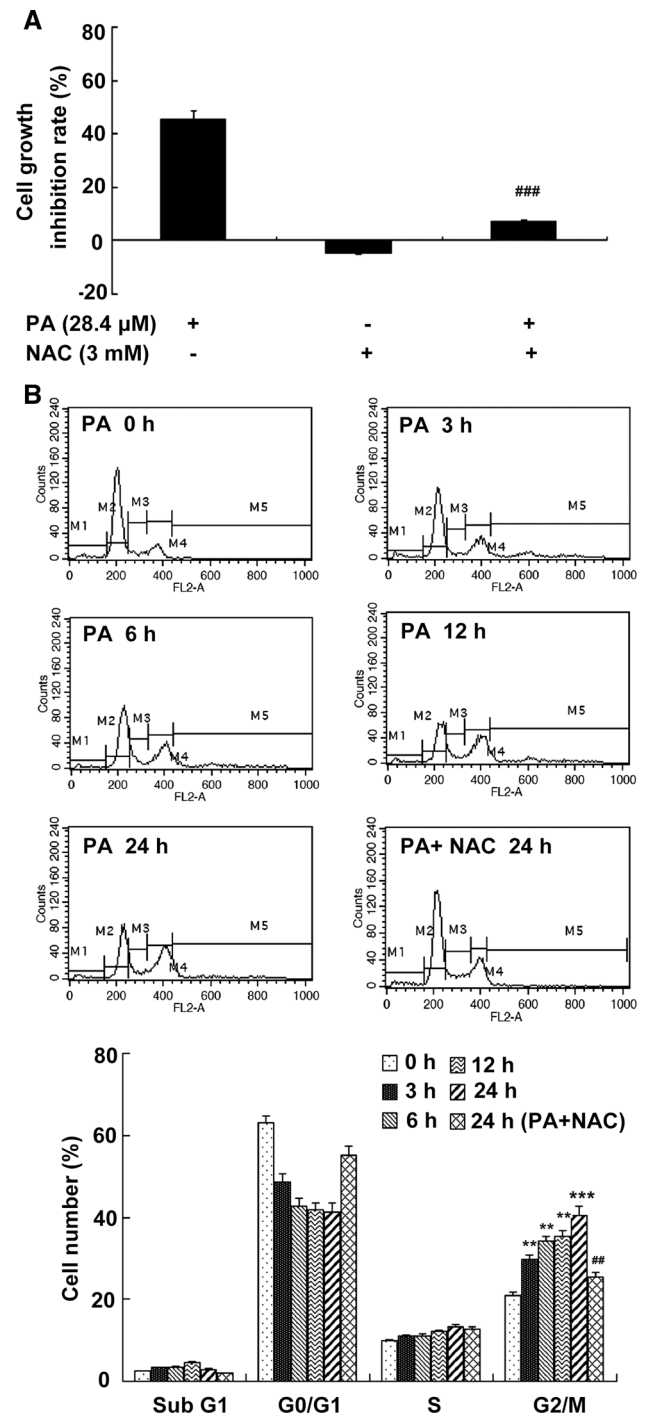


Fig. 2 PA induced G2/M cell cycle arrest in A549 cells and this effect was mediated by ROS. **a** The ROS scavenger NAC could alleviate cell growth inhibition in PA-treated cells. The cells were pretreated with or without 3 mM NAC for 1 h and then treated with $28.4 \mu\text{M}$ PA for 24 h. Cell growth inhibition was measured using the MTT assay. **b** A549 cells were cultured with $28.4 \mu\text{M}$ PA for 0, 3, 6, 12, and 24 h in the absence or presence of NAC. The DNA content was analyzed by flow cytometry using propidium iodide (PI) staining. M1: Sub G0; M2: G0/G1; M3: S; M4: G2/M. Data are shown as mean \pm SD from three independent experiments. ** $P < 0.01$, *** $P < 0.001$ versus control group ($28.4 \mu\text{M}$ PA for 0 h); ## $P < 0.01$, ### $P < 0.001$ versus A549 cells treated with $28.4 \mu\text{M}$ PA for 24 h

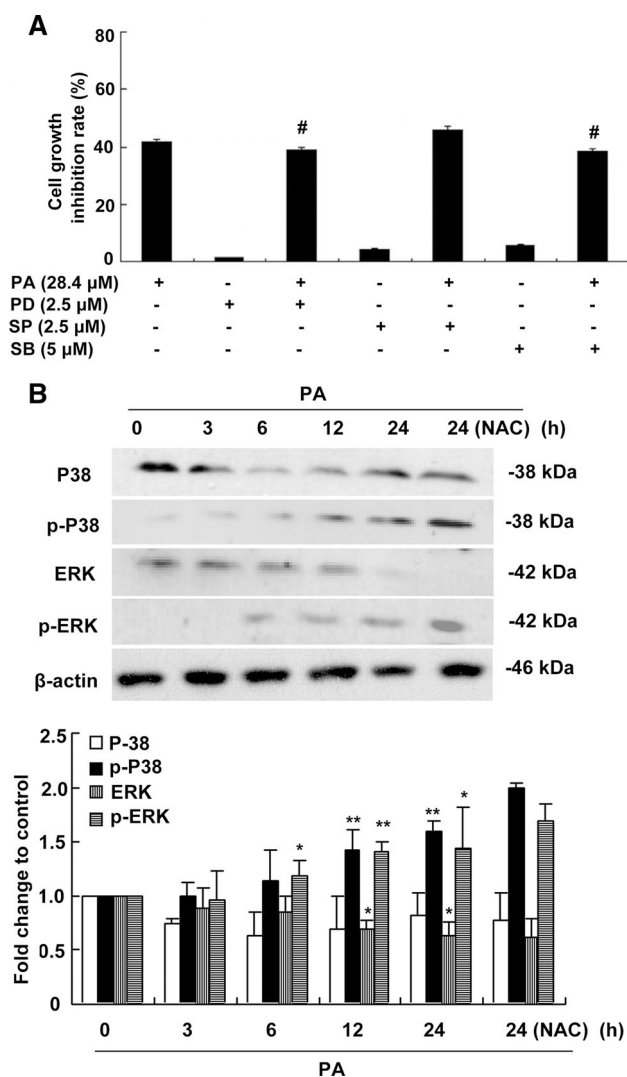


Fig. 3 Assessment of the possible signaling pathways involved in PA-induced cell cycle arrest in G2/M. **a** The cells were pretreated with the JNK inhibitor SP600125 (SP), the ERK inhibitor PD98059 (PD), or the p38 inhibitor SB203580 (SB) at the indicated concentrations for 1 h and then incubated with 28.4 μ M PA for 24 h. Cell growth inhibition was measured using the MTT assay. **b** A549 cells were treated with 28.4 μ M PA for the indicated time periods in the absence or presence of NAC, followed by Western blot analysis for the detection of ERK, p-ERK, P38, and p-P38 expressions. β -actin was used as a loading control. Data are shown as mean \pm SD from three independent experiments. * P < 0.05, ** P < 0.01 versus control group (28.4 μ M PA for 0 h); # P < 0.05 versus A549 cells treated with 28.4 μ M PA for 24 h

the expressions of ERK, p-ERK, p38, and p-p38 were detected using Western blot. As shown in Fig. 3b, ERK and p38 were triggered by PA through phosphorylation in a time-dependent manner (all P < 0.05, except at 3 h where all P > 0.05). The phosphorylation of ERK and p38, however, was not attenuated by the addition of NAC (Fig. 3b).

Effects of PD98059 and SB203580 on ROS generation and G2/M cell cycle arrest in PA-treated A549 cells

To detect the relationship between MAPK signaling and ROS generation, the intracellular ROS levels were determined using ROS-detecting fluorescent dye DCF-DA after pretreatment with PD98059 or SB203580 in PA-treated cells. As shown in Fig. 4a, the ratio of DCF-positive cells dropped from 27.6 % for PA alone to 19.6 % (P < 0.01) in the presence of SB203580 at 24 h. However, PD98059 had no significant effects on PA-treated cells.

To test the role of ERK and p38 in PA-induced cycle arrest, A549 cells were exposed to 28.4 μ M of PA for 24 h in the presence or absence of PD98059 or SB203580, and cell cycle arrest was monitored by flow cytometry. As shown in Fig. 4b, exposure of the cells to PA caused 33.4 % of the cells being arrested in the G2/M phase, compared to 17.6 % in the untreated group (P < 0.001). After pretreatment with SB203580, the proportion of cells in G2/M was reduced to 23.2 % (P < 0.001). On the other hand, exposure to PA and PD98059 did not change the proportion of cells in G2/M (P > 0.05), compared to the group treated with PA alone.

Effects of PA on cell cycle regulatory proteins in A549 cells

p53 is acknowledged as a mediator of cell cycle arrest in response to DNA damage, thus acting as a molecular ‘guardian of the genome’ [29]. p21, an inhibitor of most of the CDKs, helps to regulate the cell cycle and is an important target of p53 [29]. As shown in Fig. 5a, Western blot analysis revealed that p-p53, the active form of p53, and p21 were both notably upregulated by PA in a time-dependent manner (all P < 0.05). However, co-incubation with NAC for 24 h partially prevented this upregulation (Fig. 5a), suggesting that the production of ROS leads to the activation of p53 and p21.

The final effector in the G2/M checkpoint is the Cdc2/cyclin B1 complex, which is essential for the transition from G2 to mitosis [30]. Upon DNA damage, Cdc25c can no longer remove inhibitory phosphates from Cdc2, thus preventing the function of Cdc2/cyclin B1 complex [30]. As shown in Fig. 5b, Cdc25c, p-Cdc2, and p-cdc25c were found to be increased in a time-dependent manner after incubation with PA, along with decreases in cyclin B1 and Cdc2 expression (all P < 0.05, except at 3 h where all P > 0.05). Pretreatment with NAC efficiently inhibited the phosphorylation of Cdc2 and increased cyclin B1 and Cdc2 expressions (all P < 0.01). Cdc25c phosphorylation was increased by PA, but it was not reversed by the combined treatment of PA and NAC.

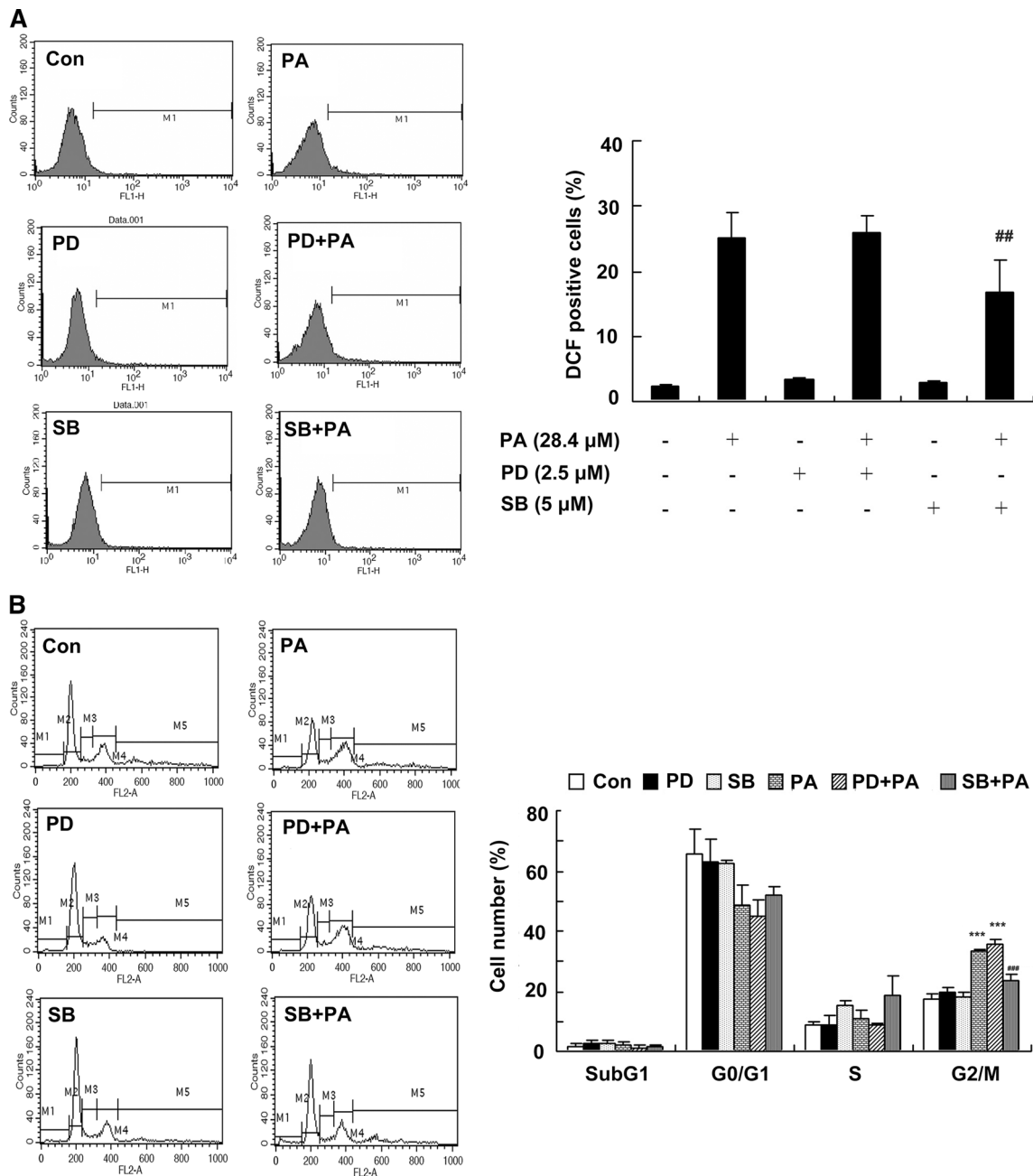


Fig. 4 Effects of ERK and p38 inhibitors on PA-induced ROS generation and G2/M cell cycle arrest in A549 cells. A549 cells were cultured in the presence of 2.5 μ M PD and 5 μ M SB for 1 h prior to the addition of 28.4 μ M PA and incubation for 24 h. **a** The generation of ROS was measured by flow cytometry using DCF-DA. **b** The DNA

content was analyzed by flow cytometry using PI staining. Data are shown as mean \pm SD from three independent experiments. *** P < 0.001 versus the control (Con) group; ## P < 0.01, ### P < 0.001 versus A549 cells treated with 28.4 μ M PA alone

Discussion

Previous studies have shown that PA extracted from *Phy-salis alkekengi* var. *franchetii* had anti-proliferation effects on a number of cancer cell lines [18, 20, 21], while lower cytotoxicity than 5-fluorouracil and paclitaxel on normal cells [20]. This study is the first to explore the effects of PA

on NSCLC cell proliferation, cell cycle distribution, and the potential mechanisms involved. Results showed that 28.4 μ M PA inhibited cell proliferation and induced G2/M cell cycle arrest in A549 cells. PA doses of 40 and 80 μ M have been shown to achieve a favorable efficacy/toxicity balance in vitro [20], but additional studies are necessary to determine the dose that could be used in vivo.

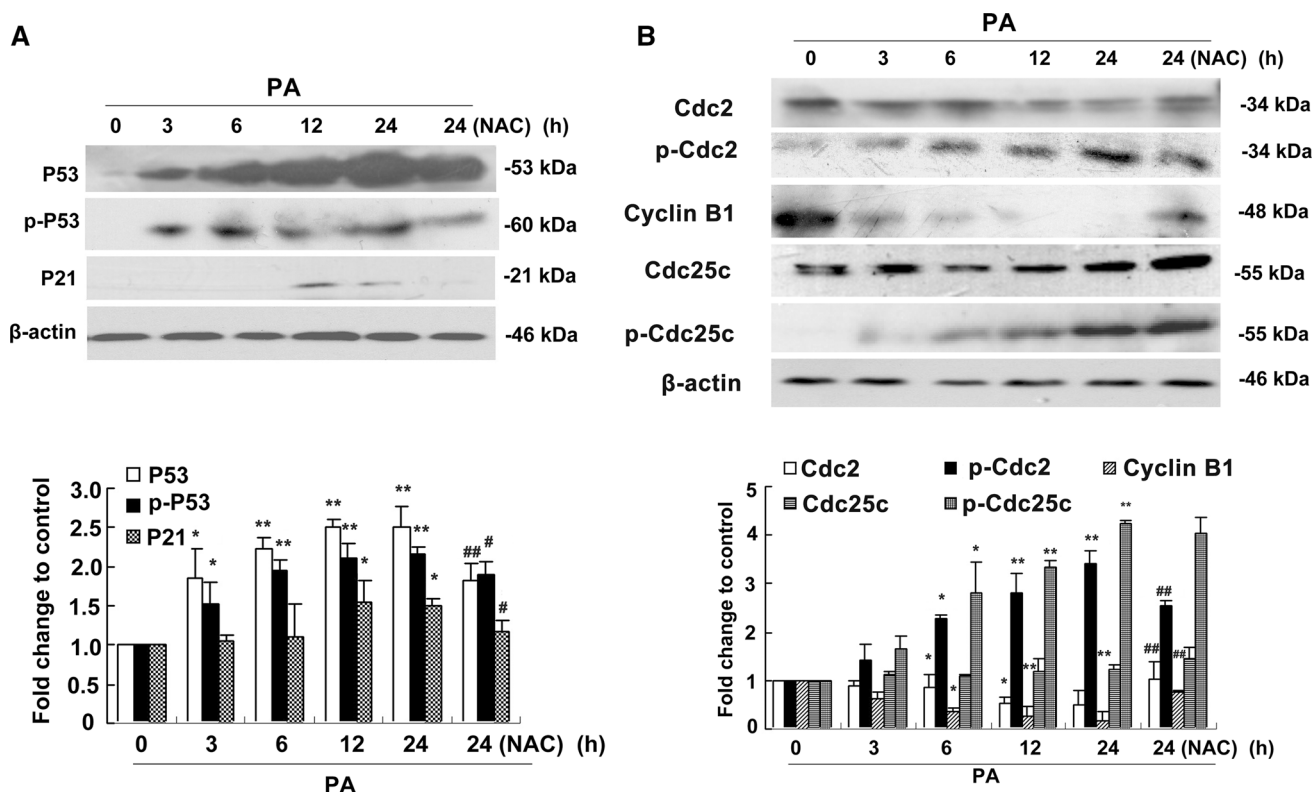


Fig. 5 PA affected the expression of proteins involved in the G2/M transition in A549 cells and this effect was mediated by ROS. A549 cells were treated with 28.4 μ M PA for the indicated time periods in the absence or presence of NAC. Western blotting was used for the detection of p53, p-p53, and p21 (a) and of Cdc2, p-Cdc2, Cyclin B1,

Cdc25c, and p-Cdc25c (b) β -actin was used as a loading control. Data are shown as mean \pm SD from three independent experiments. * P < 0.05 and ** P < 0.01 versus control group (28.4 μ M PA for 0 h); # P < 0.05, ## P < 0.01 versus A549 cells treated with 28.4 μ M PA for 24 h

MAPKs can be activated by many stress signals [31], including UV light, bacterial derivatives, growth factors, and anticancer drugs [32]. MAPKs signaling pathways regulate the eukaryotic cell cycle, and activation of MAPKs is essential for G2 to M progression [33]. The present study showed that ERK and p38 were triggered by PA through phosphorylation in a time-dependent manner, and that ERK and p38 were involved in PA-induced cell growth inhibition because PD98059 and SB203580 (inhibitors of ERK and P38, respectively) were found to be able to partly reverse PA-triggered cell growth inhibition. Furthermore, only p38 was involved in PA-induced cell cycle arrest in G2/M, while ERK was not involved. These results are similar to those obtained using other compounds activating the p38 pathway, such as 10-methoxy-9-nitrocamptothecin (MONCPT) in NSCLC A549 cells [34], secosteroid in myeloid leukemia [35], and bithionol in ovarian cancer [36], induced G2/M arrest. The involvement of these two kinases in PA-induced growth inhibition is partial, and additional studies are still necessary to identify the other actors involved in this mechanism, including but not limited to Akt [37] and miR-155 [38, 39].

ROS modulate signaling pathways, protein kinases, and transcription factors [15, 40]. Oxidative stress, DNA

damage, loss of cell function, cell cycle arrest, and apoptosis results from an excessive ROS generation [16, 17, 40]. In this study, PA stimulated the generation of ROS in a time-dependent manner, leading to G2/M cell cycle arrest in A549 cells. When incubated with NAC, a ROS scavenger, the amount of intracellular ROS was decreased, and the proportion of cells in G2/M arrest was decreased. Therefore, these results indicated that PA could induce G2/M arrest in A549 cells and this arrest was mediated by ROS. The ROS scavenger NAC almost completely blocked PA-induced growth inhibition, indicating that ROS play an important role in PA-induced A549 cell growth inhibition, possibly through apoptosis, cell cycle arrest, autophagy, or necrosis [41, 42]. The effect of NAC on PA-induced G2/M arrest is less impressive, suggesting that ROS involvement in PA-induced G2/M arrest and possible participation in other types of growth inhibition such as apoptosis, necrosis, or autophagy, also play a relevant role. However, the results of this study could not provide additional insights and additional studies are necessary to determine the other types of cell growth inhibition being involved in future.

Progression of cells from G2 to M is regulated by cyclin B/Cdc2, which has been identified as a principal

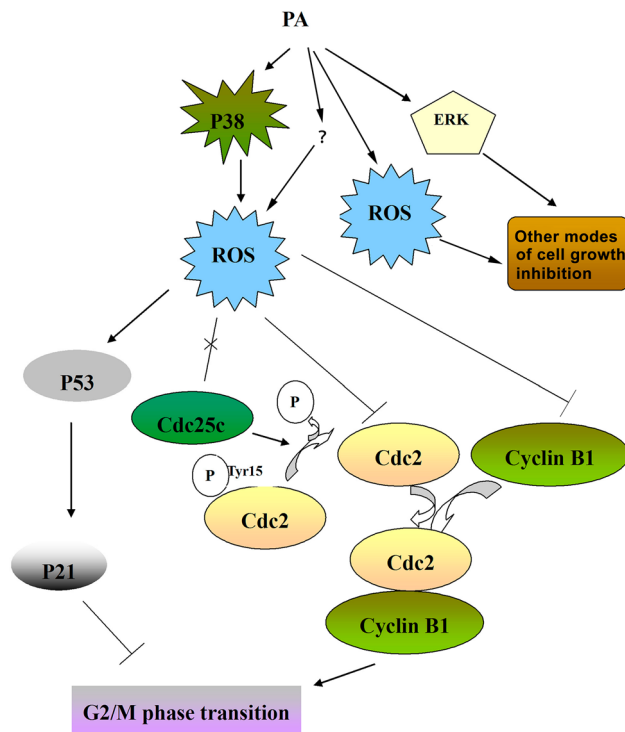


Fig. 6 Schematic representation of the signaling pathways involved in PA-induced cell cycle arrest in G2/M of A549 cells

component of the mitosis-promoting factor (MPF) [43]. p21 is a member of the CIP/KIP family, and inhibits a variety of Cdk and be regulated at the transcriptional level by p53 [44]. Cdc25c phosphatase activates cyclin B/Cdc2 by dephosphorylated Thr-14/Tyr-15 [45]. Then, activated p21 binds to and inactivates the cyclin B/Cdc2 complex that is required for cell cycle progression [46]. In this study, Western blot analysis revealed that phospho-p53, phospho-Cdc2, and p21, and Cdc25c were notably upregulated, while cyclin B1 and Cdc2 were downregulated by PA in a time-dependent manner. These effects were reversed by incubation with the ROS scavenger NAC, while the effects on Cdc25c and phospho-Cdc25c were not reversed. Therefore, these results indicate that PA could regulate some cell cycle regulatory proteins and that ROS were involved in this process, which was supported by previous one in A549 cells that cucurbitacin B induced G2/M cell cycle arrest through ROS generation and the Cha1-Cdc25c-Cdk1 and p53 pathways [47]. Since Cdc25c phosphorylation was increased by PA, but not reversed by NAC, it is probable that the effect of PA on Cdc25c is not mediated by ROS, and that other mechanisms remain to be identified.

However, the phosphorylation of ERK and P38 was not attenuated by the addition of NAC and was even increased after PA + NAC treatment. Inhibition of p38 could partly inhibit PA-induced generation of ROS and G2/M cell cycle

arrest, rather than ERK. P38 is a key mediator of cell growth, proliferation, and survival in cancer [32, 34]. In this study, it appears that p38 is the upstream effector of ROS and regulates, at least in part, G2/M arrest through the generation of ROS. It is reported that Icariside II, a natural compound, induces G2/M phase arrest by the generation of reactive oxygen species and activation of p38 and p53 in A375 human melanoma cells [48]. Additionally, a recent study has also revealed that plumbagin induced G2/M arrest, apoptosis, and autophagy in tongue squamous cell carcinoma SCC25 cells through a ROS-mediated modulation of the p38 and PI3 K/Akt/mTOR pathways [49]. However, the results of this study suggest that ERK induced cell death through another way, and the exact mechanisms were not involved. ERK is usually involved in intrinsic and extrinsic apoptotic pathways by induction of mitochondrial cytochrome *c* release or caspase-8 activation, autophagy, or permanent cell cycle arrest [50]. Further studies are needed to adequately assess the role of ERK in PA-induced cell death.

Figure 6 summarizes the effect of PA, as determined by the present study. PA might act, at least in part, through the p38 signaling pathway, which may result in increased ROS levels. ROS then disrupt the normal transition of G2 to M phase by inducing p53 and p21 activation, promoting Cdc2 phosphorylation, suppressing the expression of cyclin B1 and Cdc2, hence preventing the formation of the Cdc2/cyclin B1 complex that regulates G2 to M phase transition. Cdc25c phosphorylation was increased by PA, but not reversed by NAC. Nevertheless, the present study did not examine all factors involved in the cell response to PA. Additional comprehensive studies are necessary to address these points in future. Taken together, PA induces G2/M cell cycle arrest in NSCLC A549 cells involving in the p38 MAPK/ROS pathway. This study suggests that PA might be a promising therapeutic agent against NSCLC.

Acknowledgments This work was supported by National Natural Science Foundation of China (No. 21472138), the China Postdoctoral Science Foundation (No. 2013M541192), and the China Postdoctoral Science Special Foundation (No. 2014T70224).

Compliance with ethical standards

Conflicts of interest The authors declared that they have no conflict of interest.

References

- Kohler BA, Ward E, McCarthy BJ, Schymura MJ, Ries LA, Ehemann C, Jemal A, Anderson RN, Ajani UA, Edwards BK (2011) Annual report to the nation on the status of cancer, 1975-2007, featuring tumors of the brain and other nervous system. *J Natl Cancer Inst* 103(9):714–736

2. Ferlay J, Shin HR, Bray F, Forman D, Mathers C, Parkin DM (2010) Estimates of worldwide burden of cancer in 2008: GLOBOCAN 2008. *Int J Cancer* 127(12):2893–2917
3. Owonikoko TK, Ragin CC, Belani CP, Oton AB, Gooding WE, Taioli E, Ramalingam SS (2007) Lung cancer in elderly patients: an analysis of the surveillance, epidemiology, and end results database. *J Clin Oncol* 25(35):5570–5577
4. Pfister DG, Johnson DH, Azzoli CG, Sause W, Smith TJ, Baker S Jr, Olak J, Stover D, Strawn JR, Turrisi AT, Somerfield MR, American Society of Clinical O (2004) American Society of Clinical Oncology treatment of unresectable non-small-cell lung cancer guideline: update 2003. *J Clin Oncol* 22(2):330–353
5. Medema RH, Macurek L (2012) Checkpoint control and cancer. *Oncogene* 31(21):2601–2613
6. He H, Zang LH, Feng YS, Chen LX, Kang N, Tashiro S, Onodera S, Qiu F, Ikejima T (2013) Physalin A induces apoptosis via p53-Noxa-mediated ROS generation, and autophagy plays a protective role against apoptosis through p38-NF-kappaB survival pathway in A375-S2 cells. *J Ethnopharmacol* 148(2):544–555
7. Giacinti C, Giordano A (2006) RB and cell cycle progression. *Oncogene* 25(38):5220–5227
8. Gabrielli B, Brooks K, Pavey S (2012) Defective cell cycle checkpoints as targets for anti-cancer therapies. *Front Pharmacol* 3:9
9. Robinson MJ, Cobb MH (1997) Mitogen-activated protein kinase pathways. *Curr Opin Cell Biol* 9(2):180–186
10. Tamemoto H, Kadowaki T, Tobe K, Ueki K, Izumi T, Chatani Y, Kohno M, Kasuga M, Yazaki Y, Akanuma Y (1992) Biphasic activation of two mitogen-activated protein kinases during the cell cycle in mammalian cells. *J Biol Chem* 267(28):20293–20297
11. Pedram A, Razandi M, Levin ER (1998) Extracellular signal-regulated protein kinase/Jun kinase cross-talk underlies vascular endothelial cell growth factor-induced endothelial cell proliferation. *J Biol Chem* 273(41):26722–26728
12. Nebreda AR, Porras A (2000) p38 MAP kinases: beyond the stress response. *Trends Biochem Sci* 25(6):257–260
13. Takenaka K, Moriguchi T, Nishida E (1998) Activation of the protein kinase p38 in the spindle assembly checkpoint and mitotic arrest. *Science* 280(5363):599–602
14. Crack PJ, Taylor JM (2005) Reactive oxygen species and the modulation of stroke. *Free Radic Biol Med* 38(11):1433–1444
15. Cheng TH, Shih NL, Chen SY, Wang DL, Chen JJ (1999) Reactive oxygen species modulate endothelin-I-induced c-fos gene expression in cardiomyocytes. *Cardiovasc Res* 41(3):654–662
16. Sauer H, Wartenberg M, Hescheler J (2001) Reactive oxygen species as intracellular messengers during cell growth and differentiation. *Cell Physiol Biochem* 11(4):173–186
17. Piret B, Schoonbroodt S, Piette J (1999) The ATM protein is required for sustained activation of NF-kappaB following DNA damage. *Oncogene* 18(13):2261–2271
18. Han H, Qiu L, Wang X, Qiu F, Wong Y, Yao X (2011) Physalins A and B inhibit androgen-independent prostate cancer cell growth through activation of cell apoptosis and downregulation of androgen receptor expression. *Biol Pharm Bull* 34(10):1584–1588
19. Chinese Pharmacopoeia Committee (2010) The Pharmacopoeia of People's Republic of China, vol Vol 1. China Medical Science Press, Beijing, pp 337–338
20. He H, Zang LH, Feng YS, Wang J, Liu WW, Chen LX, Kang N, Tashiro S, Onodera S, Qiu F, Ikejima T (2013) Physalin A induces apoptotic cell death and protective autophagy in HT1080 human fibrosarcoma cells. *J Nat Prod* 76(5):880–888
21. He H, Feng YS, Zang LH, Liu WW, Ding LQ, Chen LX, Kang N, Hayashi T, Tashiro S, Onodera S, Qiu F, Ikejima T (2014) Nitric oxide induces apoptosis and autophagy; autophagy down-regulates NO synthesis in physalin A-treated A375-S2 human melanoma cells. *Food Chem Toxicol* 71:128–135
22. Qiu L, Zhao F, Jiang ZH, Chen LX, Zhao Q, Liu HX, Yao XS, Qiu F (2008) Steroids and flavonoids from *Physalis alkekengi* var. *franchetii* and their inhibitory effects on nitric oxide production. *J Nat Prod* 71(4):642–646
23. Kawabe T, Suganuma M, Ando T, Kimura M, Hori H, Okamoto T (2002) Cdc25C interacts with PCNA at G2/M transition. *Oncogene* 21(11):1717–1726
24. Berridge MV, Herst PM, Tan AS (2005) Tetrazolium dyes as tools in cell biology: new insights into their cellular reduction. *Biotechnol Annu Rev* 11:127–152
25. Zi X, Simoneau AR (2005) Flavokawain A, a novel chalcone from kava extract, induces apoptosis in bladder cancer cells by involvement of Bax protein-dependent and mitochondria-dependent apoptotic pathway and suppresses tumor growth in mice. *Cancer Res* 65(8):3479–3486
26. Bloom J, Cross FR (2007) Multiple levels of cyclin specificity in cell-cycle control. *Nat Rev Mol Cell Biol* 8(2):149–160
27. Lenaz G (2012) Mitochondria and reactive oxygen species. Which role in physiology and pathology? *Adv Exp Med Biol* 942:93–136
28. Zhang W, Liu HT (2002) MAPK signal pathways in the regulation of cell proliferation in mammalian cells. *Cell Res* 12(1):9–18
29. Reinhardt HC, Schumacher B (2012) The p53 network: cellular and systemic DNA damage responses in aging and cancer. *Trends Genet* 28(3):128–136
30. Taylor WR, Stark GR (2001) Regulation of the G2/M transition by p53. *Oncogene* 20(15):1803–1815
31. Tibbles LA, Woodgett JR (1999) The stress-activated protein kinase pathways. *Cell Mol Life Sci* 55(10):1230–1254
32. Sui X, Kong N, Ye L, Han W, Zhou J, Zhang Q, He C, Pan H (2014) p38 and JNK MAPK pathways control the balance of apoptosis and autophagy in response to chemotherapeutic agents. *Cancer Lett* 344(2):174–179
33. Wilkinson MG, Millar JB (2000) Control of the eukaryotic cell cycle by MAP kinase signaling pathways. *FASEB J* 14(14):2147–2157
34. Zhang C, Zhu H, Yang X, Lou J, Zhu D, Lu W, He Q, Yang B (2010) P53 and p38 MAPK pathways are involved in MONCPT-induced cell cycle G2/M arrest in human non-small cell lung cancer A549. *J Cancer Res Clin Oncol* 136(3):437–445
35. Zhang J, Posner GH, Danilenko M, Studzinski GP (2007) Differentiation-inducing potency of the seco-steroid JK-1624F2-2 can be increased by combination with an antioxidant and a p38MAPK inhibitor which upregulates the JNK pathway. *J Steroid Biochem Mol Biol* 105(1–5):140–149
36. Ayyagari VN, Brard L (2014) Bithionol inhibits ovarian cancer cell growth in vitro: studies on mechanism(s) of action. *BMC Cancer* 14:61
37. Iskandar K, Rezlan M, Pervaiz S (2014) Akt mediated ROS-dependent selective targeting of mutant KRAS tumors. *Free Radic Biol Med* 75(Suppl 1):S13
38. Wang P, Zhu CF, Ma MZ, Chen G, Song M, Zeng ZL, Lu WH, Yang J, Wen S, Chiao PJ, Hu Y, Huang P (2015) Micro-RNA-155 is induced by K-Ras oncogenic signal and promotes ROS stress in pancreatic cancer. *Oncotarget* 6(25):21148
39. Hou L, Chen J, Zheng Y, Wu C (2015) Critical role of miR-155/FoxO1/ROS axis in the regulation of non-small cell lung carcinomas. *Tumour Biol*, 1–8
40. Zhang Z, Leonard SS, Huang C, Vallyathan V, Castranova V, Shi X (2003) Role of reactive oxygen species and MAPKs in vanadate-induced G(2)/M phase arrest. *Free Radic Biol Med* 34(10):1333–1342

41. Ling YH, Liebes L, Zou Y, Perez-Soler R (2003) Reactive oxygen species generation and mitochondrial dysfunction in the apoptotic response to Bortezomib, a novel proteasome inhibitor, in human H460 non-small cell lung cancer cells. *J Biol Chem* 278(36):33714–33723
42. Wang WL, Healy ME, Sattler M, Verma S, Lin J, Maulik G, Stiles CD, Griffin JD, Johnson BE, Salgia R (2000) Growth inhibition and modulation of kinase pathways of small cell lung cancer cell lines by the novel tyrosine kinase inhibitor STI 571. *Oncogene* 19(31):3521–3528
43. Arion D, Meijer L, Brizuela L, Beach D (1988) cdc2 is a component of the M phase-specific histone H1 kinase: evidence for identity with MPF. *Cell* 55(2):371–378
44. Bates S, Ryan KM, Phillips AC, Vousden KH (1998) Cell cycle arrest and DNA endoreduplication following p21Waf1/Cip1 expression. *Oncogene* 17(13):1691–1703
45. Strausfeld U, Labbe JC, Fesquet D, Cavadore JC, Picard A, Sadhu K, Russell P, Doree M (1991) Dephosphorylation and activation of a p34cdc2/cyclin B complex in vitro by human CDC25 protein. *Nature* 351(6323):242–245
46. Harper JW, Adami GR, Wei N, Keyomarsi K, Elledge SJ (1993) The p21 Cdk-interacting protein Cip1 is a potent inhibitor of G1 cyclin-dependent kinases. *Cell* 75(4):805–816
47. Guo J, Wu G, Bao J, Hao W, Lu J, Chen X (2014) Cucurbitacin B induced ATM-mediated DNA damage causes G2/M cell cycle arrest in a ROS-dependent manner. *PLoS ONE* 9(2):e88140
48. Wu J, Song T, Liu S, Li X, Li G, Xu J (2015) Icariside II inhibits cell proliferation and induces cell cycle arrest through the ROS-p38-p53 signaling pathway in A375 human melanoma cells. *Mol Med Rep* 11(1):410–416
49. Pan ST, Qin Y, Zhou ZW, He ZX, Zhang X, Yang T, Yang YX, Wang D, Qiu JX, Zhou SF (2015) Plumbagin induces G2/M arrest, apoptosis, and autophagy via p38 MAPK- and PI3 K/Akt/mTOR-mediated pathways in human tongue squamous cell carcinoma cells. *Drug Des Devel Ther* 9:1601–1626
50. Cagnol S, Chambard JC (2010) ERK and cell death: mechanisms of ERK-induced cell death—apoptosis, autophagy and senescence. *FEBS J* 277(1):2–21